

Photons in a cold axion background and strong magnetic fields: polarimetric consequences

Domènec Espriu¹ and Albert Renau¹

¹Departament d'Estructura i Constituents de la Matèria,

Institut de Ciències del Cosmos (ICCUB),

Universitat de Barcelona, Martí Franquès 1, 08028 Barcelona, Spain

Abstract

In this work we analyze the propagation of photons in an environment where a strong magnetic field (perpendicular to the photon momenta) coexists with an oscillating cold axion background with the characteristics expected from dark matter in the galactic halo. Qualitatively, the main effect of the combined background is to produce a three-way mixing among the two photon polarizations and the axion. It is interesting to note that in spite of the extremely weak interaction of photons with the cold axion background, its effects compete with those coming from the magnetic field in some regions of the parameter space. We determine (with one plausible simplification) the proper frequencies and eigenvectors as well as the corresponding photon ellipticity and induced rotation of the polarization plane that depend both on the magnetic field and the local density of axions. We also comment on the possibility that some of the predicted effects could be measured in optical table-top experiments.

I. INTRODUCTION

Originally introduced to solve the strong CP problem [1–3], axions are an attractive and viable candidate for dark matter (DM) [4–7]. The axion is the Goldstone boson associated with the spontaneous breaking of the $U(1)_{PQ}$ symmetry [1–3]. After the QCD phase transition, instanton effects induce a potential on the axion field, giving it a mass m_a . Astrophysical and cosmological constraints (see below) force this mass to be quite small. Yet, the axion provides cold dark matter, as it is not produced thermically. If the axion background field is initially misaligned (not lying at the bottom of the instanton-induced potential), at late times it oscillates coherently as

$$a_b(t) = a_0 \sin m_a t, \quad (1)$$

where the amplitude, a_0 , is related to the initial misalignment angle. The oscillation of the axion field has an approximately constant (i.e. space-independent) energy density $\rho = \frac{1}{2}a_0^2 m_a^2$, which contributes to the total energy of the universe¹. This constitutes the cold axion background (CAB for short). There are suggestions that axions could actually form a Bose-Einstein condensate (BEC) [8].

Axions couple to photons through the term

$$\mathcal{L}_{a\gamma\gamma} = g_{a\gamma\gamma} \frac{\alpha}{2\pi} \frac{a}{f_a} F_{\mu\nu} \tilde{F}^{\mu\nu}, \quad (2)$$

where the coefficient $g_{a\gamma\gamma}$ depends on the model². However, most of them [9–12] give $g_{a\gamma\gamma} \simeq 1$. For the present discussion this is all that matters. The near-universality of the axion-photon coupling makes it the best candidate to explore axion physics.

This coupling is severely bounded. The lower limit $f_a > 10^7$ GeV coming from astrophysical considerations seems now well established. If one assumes that axions are the main ingredient of DM, there is also an upper bound: $f_a < 3 \cdot 10^{11}$ GeV. See Ref. [7] and references therein for an explanation of the above bounds. These values of f_a make the axion very weakly coupled and imply a very long lifetime, of the order of 10^{24} years or more; see e.g. Ref. [13]. In the case of Peccei-Quinn axions (i.e. solving the strong CP problem)

¹ This density is not really constant, as DM tends to concentrate in galactic halos. Nevertheless it is assumed to change over very large scales, so for our purposes it suffices to treat it as a constant.

² Sometimes a dimensionful coupling constant $G_{a\gamma\gamma} \propto \frac{1}{f_a}$ is used instead. Our $g_{a\gamma\gamma}$ is dimensionless.

the approximate relation $f_a m_a \simeq f_\pi m_\pi$ should hold and therefore cosmology considerations place the axion mass in the range $10^{-1} - 10^{-6}$ eV. For other axion-like particles, not related to the strong CP problem, there is no such relation between m_a and f_a and the range of possible values is more open, although they are less motivated from a physical point of view.

Axions could also couple to matter, although in this case the coupling is much more model dependent. The coupling is so small that their detection is very difficult. Nevertheless, some of the best bounds on axion masses and couplings come from the study of abnormal cooling in white dwarfs due to axion emission [14].

When dealing with axions and their possible cosmological relevance, there are several separate issues that have to be addressed. The first one is whether a particle with the properties of the axion exists or not. This is what experiments such as CAST [15], IAXO [16] or ALPS [17] are addressing directly. If the axion does exist and its mass happens to be in the relevant range for cosmology we would have a strong hint that axions may serve as valid DM candidates. Of course for axions to be the main component of DM they also have to be present in a sufficient amount.

The mechanism of vacuum misalignment and the subsequent redshift of momenta suggest that it is natural for axions to remain coherent (or very approximately so) over relatively long distances, perhaps even forming a BEC as has been suggested. Thus one should expect not only that the momentum of individual axions satisfies the condition $k \ll m_a$ as required from cold DM but also all that axions oscillate in phase, rather than incoherently, at least locally. In addition one needs that the modulus of the axion field is large enough to account for the DM density.

Finding an axion particle with the appropriate characteristics is not enough to demonstrate that a CAB exists. Detecting the coherence of the axion background and hence validating the misalignment proposal is therefore not within reach of any of the above experiments.

The ADMX Phase II experiment [18] tries to detect axions in the Galaxy dark matter halo that, under the influence of a strong magnetic field, would convert to photons with a frequency equal to the axion mass in a resonant cavity. This experiment is sensitive to the local axion density, the probability of a positive detection being proportional to the latter. In order to get a significant signal the axion field has to be significantly constant at length scales comparable to the cavity size. ADMX is therefore sensitive to the CAB. The experiment

claims sensitivity to axions in the approximate mass range 10^{-6} eV to 10^{-5} eV and this is also the range of momenta at which the axion background field can be significantly probed in such an experiment.

Looking for the collective effects on photon propagation resulting from the presence of a CAB is another possible way of investigating whether a CAB is present at the scales probed by the experiment. Of course we do not anticipate large or dramatic effects given the presumed smallness of the photon-to-axion coupling and the low density background that a CAB would provide. However, interferometric and polarimetric techniques are very powerful and it is interesting to explore the order of magnitude of the different effects in this type of experiments. Potentially, photons can also probe the CAB structure in different ranges of momenta. In addition, precise photon measurements could in principle check the coherence of the oscillations over a variety of distances. Discussing in detail the effects of a CAB on photons is the purpose of the present paper.

Several studies on the influence of axions on photon propagation at cosmological scales exist[19–22]. The consequences are only visible for extremely low mass axions, such as the ones hypothetically produced in string theory scenarios[23]. We do not consider very light axions here in detail as their masses do not fall into the favoured range but exploring such small masses might be of interest too.

It is worth noting that a CAB introduces via its time dependence some amount of Lorentz-invariance violation in photon physics; the term (2) does actually modify the photon dispersion relation and it has somewhat exotic consequences. For instance, in Ref. [24] we showed how this modification of the dispersion relation allows the emission of a photon by a cosmic ray, a process forbidden due to conservation of energy and momentum in a Lorentz-invariant theory. In Ref. [25] we computed the amount of energy radiated by this process and found it to be non-negligible, although the normal synchrotron radiation background makes its detection very challenging.

In Ref. [26] we found that some photon wave numbers are actually forbidden in a CAB, as a consequence of its time dependence. This striking result is an unavoidable and direct consequence of the periodicity of the CAB oscillations. In the subsequent we study the actual width of these gaps that, not surprisingly, turns out to be extremely narrow for axions of cosmological relevance.

The consequences of the mere existence of axions as propagating degrees of freedom on

photon propagation have been studied for a long time and are well understood. It is well known that photons polarized in a direction perpendicular to the magnetic field are not affected by the existence of axions [27, 28] but photons polarized in the parallel direction mix with them. As a consequence there is a small rotation in the polarization plane due to photon-axion mixing as well as a change in the ellipticity [29]. In Ref. [26] we showed that a similar effect exists even without a magnetic field when a CAB is present except that now it involves the two photon helicities.

Throughout this work we will see that the effects of the CAB on the propagation of photons are extremely small, so it is quite pertinent to question whether these effects could be experimentally measured. The answer is surely negative with present day experimental capabilities but some effects are not ridiculously small either to be discarded from the outset: the effects of a coherent CAB are in some cases quite comparable to, or even larger than, the influence of axions as mere propagating degrees of freedom, which have been profusely studied before. They might even be comparable to non-linear QED effects, which have also been actively sought for experimentally. Therefore we think it is legitimate to present this study in view of the physical relevance of the presumed existence of a CAB as a dark matter candidate.

This work is a continuation of Ref. [26] and some overlap is unavoidable to be reasonably self-contained. In section II we review the problem and derive the equations of motion for the axion and photon in the presence of both backgrounds, both for linear and circular polarization bases for the photon. We also review there the range of relevant values for the intervening parameters. In section III we discuss the results for the case of no magnetic field, when there is no photon-axion conversion but the CAB still mixes the two photon helicities. In Ref. [26] we found that some gaps in the photon momenta were present due to the time periodicity of the CAB. We complement this discussion now by deriving the precise location and width of these momentum gaps. In section IV we study the consequences that the combined background has on photon wave-numbers and polarizations. In section V we explore the consequences of the change in the plane of polarization of the photons in the presence of the CAB, making use of the photon propagator derived in a combined CAB and constant magnetic field that was derived in Ref. [26]. We also correct some approximations that were made in Ref. [26] and that turn out not to be correct for the relevant range of masses, magnetic fields and CAB densities. We have also made an effort in presenting the

new the results in a standard notation, more suitable for optical experiments. The technical details are given in a detailed appendix. A short summary of some of our results was already presented in Ref. [30].

II. EQUATIONS OF MOTION OF THE AXION-PHOTON SYSTEM

The Lagrangian density describing axions and photons consists of the usual kinetic terms plus the interaction term (2)

$$\mathcal{L} = \frac{1}{2}\partial_\mu a \partial^\mu a - \frac{1}{2}m_a^2 a^2 - \frac{1}{4}F_{\mu\nu}F^{\mu\nu} + \frac{g}{4}aF_{\mu\nu}\tilde{F}^{\mu\nu}, \quad (3)$$

where we have rewritten the axion-photon coupling as $g = g_{a\gamma\gamma}\frac{2\alpha}{\pi f_a}$. We are not considering the non-linear effects due to the Euler-Heisenberg Lagrangian [31, 32] that actually can provide some modifications in the polarization plane. Later we shall discuss their relevance.

We decompose the fields as a classical piece describing the backgrounds (external magnetic field \vec{B} and a CAB as given in (1) plus quantum fluctuations describing the photon and the axion particles, e.g. $a \rightarrow a_b + a$. For the (quantum) photon field, we work in the Lorenz gauge, $\partial_\mu A^\mu = 0$, and use the remaining gauge freedom to set $A^0 = 0$. The equations of motion are

$$\begin{aligned} (\partial_\mu \partial^\mu + m_a^2)a + gB^i \partial_t A_i &= 0, \\ \partial_\mu \partial^\mu A^i + gB^i \partial_t a + \eta \epsilon^{ijk} \partial_j A_k &= 0, \end{aligned} \quad (4)$$

where $\eta = g\partial_t a_b$. We neglect the space derivatives of a_b thereby assuming homogeneity of the axion background, at least at the scale of the photon momentum and translational invariance. Since η is time-dependent, we make a Fourier transform with respect to the spatial coordinates only,

$$\phi(t, \vec{x}) = \int \frac{d^3k}{(2\pi)^3} e^{i\vec{k}\cdot\vec{x}} \hat{\phi}(t, \vec{k}), \quad (5)$$

and get the equations

$$\begin{aligned} (\partial_t^2 + \vec{k}^2 + m_a^2)\hat{a} + gB^i \partial_t \hat{A}_i &= 0, \\ (\partial_t^2 + \vec{k}^2)\hat{A}^i + gB^i \partial_t \hat{a} + i\eta \epsilon^{ijk} k_j \hat{A}_k &= 0. \end{aligned} \quad (6)$$

As can be seen, the presence of a magnetic field mixes the axion with the photon. To proceed further, we write the photon field as

$$\hat{A}_\mu(t, \vec{k}) = \sum_\lambda f_\lambda(t) \varepsilon_\mu(\vec{k}, \lambda), \quad (7)$$

where ε_μ are the polarization vectors and $f_\lambda(t)$ are the functions we will have to solve for. If we choose a linear polarization basis for the photon, the equations are, in matrix form,

$$\begin{pmatrix} \partial_t^2 + k^2 + m_a^2 & -ib\partial_t & 0 \\ -ib\partial_t & \partial_t^2 + k^2 & -\eta(t)k \\ 0 & -\eta(t)k & \partial_t^2 + k^2 \end{pmatrix} \begin{pmatrix} \hat{a} \\ if_\parallel \\ f_\perp \end{pmatrix} = \begin{pmatrix} 0 \\ 0 \\ 0 \end{pmatrix}, \quad (8)$$

where $k = |\vec{k}|$ and $b = g|\vec{B}^\perp|$, where \vec{B}^\perp is the component of the magnetic field perpendicular to the momentum (the parallel component does not affect propagation at all if the Euler-Heisenberg piece is neglected). The subscripts \parallel and \perp refer to parallel or perpendicular to this \vec{B}^\perp .

In a circular polarization basis, defining

$$f_\pm = \frac{f_\parallel \pm if_\perp}{\sqrt{2}}, \quad (9)$$

the equations take the form

$$\begin{pmatrix} \partial_t^2 + k^2 + m_a^2 & i\frac{b}{\sqrt{2}}\partial_t & i\frac{b}{\sqrt{2}}\partial_t \\ i\frac{b}{\sqrt{2}}\partial_t & \partial_t^2 + k^2 + \eta(t)k & 0 \\ i\frac{b}{\sqrt{2}}\partial_t & 0 & \partial_t^2 + k^2 - \eta(t)k \end{pmatrix} \begin{pmatrix} i\hat{a} \\ f_+ \\ f_- \end{pmatrix} = \begin{pmatrix} 0 \\ 0 \\ 0 \end{pmatrix}. \quad (10)$$

As we see from the previous expressions, the presence of a CAB changes in a substantial way the mixing of photons and axions. Now all three degrees of freedom are involved.

A difference in the approach between this work and Ref. [33] is worth noting. In going from (4) to (6) we have performed a Fourier transform in space, but not in time, because the magnetic field is homogeneous but $\eta(t)$ is time-dependent. Equation (4) in Ref. [33], however, uses a transform in time rather than in space because the CAB is not considered.

There are several ways to deal with the periodic CAB. One possibility is to try to treat it exactly. Unfortunately this unavoidably leads to the appearance of Mathieu functions due to the sinusoidal variation of the background and the analysis becomes extremely involved. On the other hand, the substantial ingredient in the problem is the existence of periodicity itself and the fine details are not so relevant³. Therefore to keep the discussion manageable, we approximate the sinusoidal variation of the axion background $a_b(t)$ in (1) by a piecewise

³ Recall that the generic appearance of bands in the energy levels of a solid relies on the periodicity of the potential and not on its precise details.

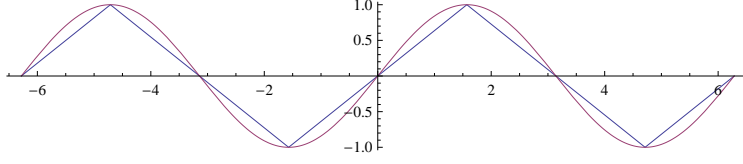


FIG. 1: $a_b(m_a t)/a_0$ and its approximating function.

linear function, see figure 1. Since $\eta(t)$ is proportional to the time derivative of $a_b(t)$, in this approximation it is a square-wave function, alternating between intervals where $\eta = \eta_0$ and $\eta = -\eta_0$ with a period $2T = 2\pi/m_a$. Here, $\eta_0 = \frac{2}{\pi} g a_0 m_a = g_{a\gamma\gamma} \frac{4\alpha}{\pi^2} \frac{a_0 m_a}{f_a}$.

A brief numerical discussion of the parameters involved in the problem and their relative importance is now in order. The bound on f_a implies one on g . Taking $g_{a\gamma\gamma}$ of $\mathcal{O}(1)$ the range $f_a = 10^7 - 10^{11}$ GeV translates to $g = 10^{-18} - 10^{-22}$ eV $^{-1}$. Assuming a halo DM density of $\rho = 10^{-4}$ eV 4 [34] this means that $\eta_0 = 10^{-20} - 10^{-24}$ eV. When working with natural units and magnetic fields it is useful to know that 1 T \approx 195 eV 2 . To have a reference value, a magnetic field of 10 T implies the range $b = 10^{-15} - 10^{-19}$ eV, for $f_a = 10^7 - 10^{11}$ GeV.

Finally, let us now comment on the relevance of the contribution of the Euler-Heisenberg pieces compared to the ones retained in the description provided by (3). As it is known (see e.g. Ref. [27, 28]) an external magnetic field perpendicular to the photon motion contributes, via the Euler-Heisenberg terms, to the mixing matrices, affecting the (2,2) and (3,3) entries of (8) and (10). They modify the k^2 terms with corrections of order $10^{-2} \times \alpha^2 \times (B^2/m_e^4)$, where m_e is the electron mass, leading to birefringence and therefore to ellipticity. For magnetic fields of ~ 10 T this gives a contribution of order 10^{-21} that may be comparable to axion-induced effects for large magnetic fields, particularly if f_a is very large, or to the effects from the CAB (which for $k \sim 1$ eV are in the range $10^{-20} - 10^{-24}$). Since there is no new physics involved in the contribution from the Euler-Heisenberg Lagrangian, in order to facilitate the analysis we will not consider it here. In any case given the smallness of the Euler-Heisenberg and the axion effects, they can safely be assumed to be additive [27, 28]. The relevant modifications due to the Euler-Heisenberg term can be found in Refs. [27, 28] and [35].

Of course, the effects of the Euler-Heisenberg Lagrangian are absent or negligible if there is no magnetic field or if it is relatively weak, and we will see that for a range of parameters the effect of a CAB might be comparable to the former.

III. NO MAGNETIC FIELD: FORBIDDEN WAVELENGTHS

If there is no magnetic field ($b = 0$, $\eta_0 \neq 0$) the axion and the photon are no longer mixed. We explored this situation in Ref. [26] and we will summarize the main results here and complete the discussion.

Because $\eta(t)$ does mix the two linear polarizations, in this case it is useful to choose the circular polarization basis, which diagonalizes the system. The solution is, for a given interval, $f_{\pm}(t) = e^{i\omega_{\pm}t}$, $\omega_{\pm} = \sqrt{k^2 \pm \eta_0 k}$. Of course, when $\eta(t)$ changes sign the solutions are interchanged as well. The way to solve this is to write $f_{\pm}(t) = e^{i\Omega t} g_{\pm}(t)$ and demand that $g_{\pm}(t)$ have the same periodicity as $\eta(t)$. After elementary quantum mechanical considerations, periodicity of the modulus of the wave-function imposes the condition

$$\cos(2\Omega T) = \cos(\omega_+ T) \cos(\omega_- T) - \frac{\omega_+^2 + \omega_-^2}{2\omega_+ \omega_-} \sin(\omega_+ T) \sin(\omega_- T). \quad (11)$$

This condition implies the existence of momentum gaps: some values of k admit no solution for Ω , much like some energy bands are forbidden in a semiconductor. Here, however, the roles of momentum and energy are exchanged, since the periodicity is in time, rather than in space. The solutions are shown in an $\Omega(k)$ plot in figure 2 for two values of the ratio η_0/m_a . One of the ratios shown is unreasonably large, in order to show clearly the existence of the gaps.

Let us now discuss the width of these gaps, an issue that was not studied in Ref. [26] in detail. The first order in η_0 drops from (11) but to second order it reads

$$\cos(2\Omega T) = \cos(2kT) + \frac{\eta_0^2}{4k^2} [-1 + \cos(2kT) + kT \sin(2kT)] \quad (12)$$

(recall that $T = \pi/m_a$). There is no solution when the r.h.s. of this expression becomes larger than one. The gaps are approximately located at

$$k_n = \frac{n m_a}{2}, \quad n \in \mathbb{N} \quad (13)$$

and their width is

$$\Delta k \sim \begin{cases} \frac{\eta_0}{n\pi} & \text{for } n \text{ odd} \\ \frac{\eta_0^2}{2n m_a} & \text{for } n \text{ even} \end{cases}. \quad (14)$$

These results agree well with the exact results as can be easily seen in the left side of figure 2. Unfortunately we are not aware of any way of detecting such a tiny forbidden band for

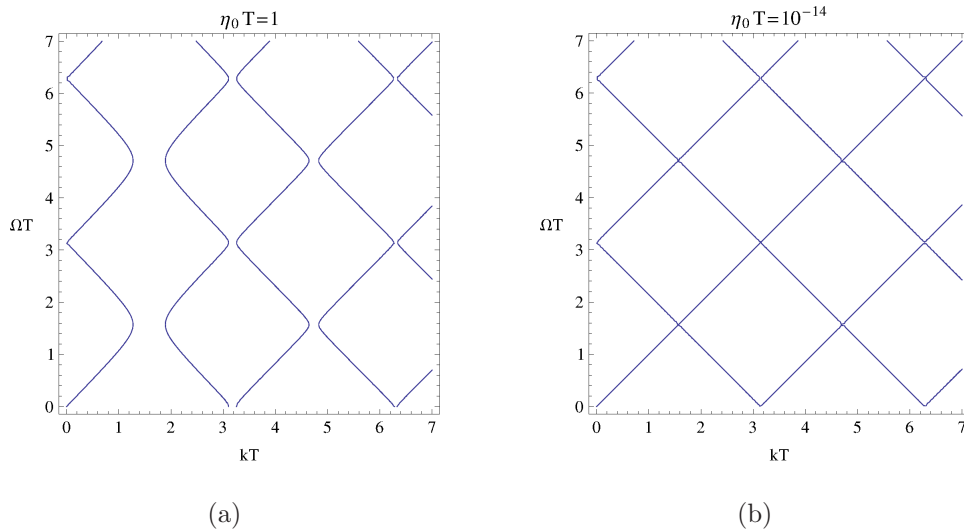


FIG. 2: Plot of the solutions to the gap equation. In the left figure the value for the ratio η_0/m_a is unreasonably large and it is presented here only to make the gaps in the photon momentum clearly visible.

the range of values of η_0 previously quoted (10^{-20} eV or less) that correspond to the allowed values of f_a .

It may be interesting to think what would happen if one attempts to produce a ‘forbidden’ photon, i.e. one whose momentum falls in one of the forbidden bands. A photon with such a wave number is ‘off-shell’ and as such it will always decay. For instance, it could decay into three other photons with appropriately lower energies. However, because the off-shellness is so small (typically 10^{-20} eV or less) it could live for a long time as a metastable state, travelling distances commensurable with the solar system. For more technical details see e.g. Ref. [36].

We realize that the small bandwidth of the forbidden momentum bands make them unobservable in practice. However their mere existence is of theoretical interest. Conclusions might be different for other axion-like backgrounds.

IV. PROPER MODES IN A MAGNETIC FIELD AND AXION BACKGROUND

In the presence of a magnetic field, but no CAB ($b \neq 0$, $\eta_0 = 0$) there is no longer a time dependence in the coefficients of the equations, so we can Fourier transform with respect to

time as well. We find the following dispersion relations:

$$\begin{aligned}\omega_a^2 &= k^2 + \frac{m_a^2 + b^2}{2} + \frac{1}{2}\sqrt{(m_a^2 + b^2)^2 + 4b^2k^2} \approx (k^2 + m_a^2) \left(1 + \frac{b^2}{m_a^2}\right) \\ \omega_1^2 &= k^2 + \frac{m_a^2 + b^2}{2} - \frac{1}{2}\sqrt{(m_a^2 + b^2)^2 + 4b^2k^2} \approx k^2 \left(1 - \frac{b^2}{m_a^2}\right) \\ \omega_2^2 &= k^2,\end{aligned}\tag{15}$$

where the \approx symbol indicates the limit $\frac{bk}{m_a^2} \ll 1$. These results are well known [29]. We have identified as corresponding to ‘photons’ the two modes that if $b = 0$ reduce to the two usual polarization modes. The third frequency corresponds predominantly to the axion (or axion-like particle), but of course it has also a small photon component as the \parallel polarized photon mixes with the axion.

If laser light of frequency ω is injected into a cavity, the different components will develop different wave-numbers resulting in the appearance of changes in the plane of polarization (ellipticity and rotation) unless the photon polarization is initially exactly parallel or exactly perpendicular to the magnetic field. We will review these effects later. From the above expressions it would appear that the relevant figure of merit to observe distortions with respect the unperturbed photon propagation is the ratio $\frac{b^2}{m_a^2}$ and this is indeed true at large times or distances (actually for $x \gg \frac{\omega}{m_a^2}$). This number is of course very small, typically 10^{-28} for the largest conceivable magnetic fields (note that this ratio is actually independent of f_a and m_a provided that we are considering Peccei-Quinn axions.)

Laser interferometry is extremely precise and Michelson-Morley type experiments are capable of achieving a relative error as small as 10^{-17} using heterodyne interferometry techniques[37, 38] and the PVLAS collaboration claims that a sensitivity of order 10^{-20} in the difference of refraction indices is ultimately achievable [39] (see also Ref. [40]). In spite of this the above figure seems way too small to be detectable.

Let us now explore the situation where both the CAB and the magnetic field are present. We choose to work with the linear polarization basis. Again, in each time interval we can define $(a, if_{\parallel}, f_{\perp}) = e^{i\omega t}(x, iX_{\parallel}, X_{\perp})$. Then the equations in matrix form are

$$\begin{pmatrix} -\omega^2 + k^2 + m_a^2 & \omega b & 0 \\ \omega b & -\omega^2 + k^2 & -\eta_0 k \\ 0 & -\eta_0 k & -\omega^2 + k^2 \end{pmatrix} \begin{pmatrix} x \\ iX_{\parallel} \\ X_{\perp} \end{pmatrix} = \begin{pmatrix} 0 \\ 0 \\ 0 \end{pmatrix},\tag{16}$$

and involve a full three-way mixing as previously mentioned. The proper frequencies of the

system turn out to be

$$\begin{aligned}\omega_a^2 &= k^2 + \frac{m_a^2 + b^2}{3} + 2\sqrt{Q} \cos \phi, \\ \omega_1^2 &= k^2 + \frac{m_a^2 + b^2}{3} - \sqrt{Q} (\cos \phi + \sqrt{3} \sin \phi), \\ \omega_2^2 &= k^2 + \frac{m_a^2 + b^2}{3} - \sqrt{Q} (\cos \phi - \sqrt{3} \sin \phi),\end{aligned}\tag{17}$$

where

$$\begin{aligned}Q &= \left(\frac{m_a^2 + b^2}{3} \right)^2 + \frac{1}{3} k^2 (b^2 + \eta_0^2), \\ \phi &= \frac{1}{3} \arctan \frac{\sqrt{Q^3 - R^2}}{R}, \\ R &= \frac{1}{54} (m_a^2 + b^2) [2m^4 + b^2(9k^2 + 4m_a^2 + 2b^2)] - \frac{1}{6} \eta_0^2 k^2 (2m_a^2 - b^2).\end{aligned}\tag{18}$$

It can be observed that they depend only on even powers of η_0 , so they are not altered when $\eta(t)$ changes sign. According to the discussion at the end of section II the limit $\eta_0 \ll b \ll \{m_a, k\}$ is quite reasonable. The approximate expressions for the proper frequencies in this limit are⁴

$$\begin{aligned}\omega_a^2 &\approx (k^2 + m_a^2) \left(1 + \frac{b^2}{m_a^2} \right), \\ \omega_1^2 &\approx k^2 - k \sqrt{\eta_0^2 + \left(\frac{b^2 k}{2m_a^2} \right)^2} - \frac{b^2 k^2}{2m_a^2}, \\ \omega_2^2 &\approx k^2 + k \sqrt{\eta_0^2 + \left(\frac{b^2 k}{2m_a^2} \right)^2} - \frac{b^2 k^2}{2m_a^2}.\end{aligned}\tag{19}$$

Corresponding to each frequency, the eigenvectors that solve the system are

$$\omega_a : \begin{pmatrix} 1 \\ \frac{b\sqrt{k^2 + m_a^2}}{m_a^2} \\ -\frac{\eta_0 b k \sqrt{k^2 + m_a^2}}{m_a^4} \end{pmatrix}, \quad \omega_1 : \begin{pmatrix} -\frac{bk}{m_a^2} \\ 1 \\ \varepsilon \end{pmatrix}, \quad \omega_2 : \begin{pmatrix} \frac{bk}{m_a^2} \varepsilon \\ -\varepsilon \\ 1 \end{pmatrix},\tag{20}$$

where

$$\varepsilon = \frac{\eta_0}{\sqrt{\eta_0^2 + \left(\frac{b^2 k}{2m_a^2} \right)^2} + \frac{b^2 k}{2m_a^2}}.\tag{21}$$

⁴ Extreme care has to be exercised when using approximate formulae based on series expansions in b or η_0 because there is a competition among dimensionful quantities, several of which take rather small values.

Note that the above eigenvectors are written in the basis described in (9) that includes an imaginary unit for the parallel component. Therefore the eigenvectors for $\omega_{1,2}$ correspond to photon states elliptically polarized with ellipticity ⁵ $|\varepsilon|$. In addition, unless exactly aligned to the magnetic field there will be a change in the angle of polarization. We will return to this in section V.

We also note that the above value for ε corresponds to the ellipticity of the eigenmodes. In section V we will discuss the evolution of the ellipticity of photon state that is initially linearly polarized.

Let us now try to get some intuition on the relevance of the different magnitudes entering in the expressions. There are two different limits we can study, depending of which term in the square root in (21) dominates. If $\frac{|\eta_0|}{k} \ll \frac{b^2}{2m_a^2}$ we have $\varepsilon \approx \frac{\eta_0 m_a^2}{b^2 k}$. The ellipticity of the eigenmodes is small, so the proper modes are almost linearly polarized photons. In the case $\frac{|\eta_0|}{k} \gg \frac{b^2}{2m_a^2}$ we have $\varepsilon \approx \text{sign}(\eta_0) \left(1 - \frac{b^2 k}{2|\eta_0| m_a^2}\right)$. Now the ellipticity of the eigenmodes is close to 1 so the proper modes are almost circularly polarized. We see that while the proper frequencies depend only on the square of η_0 (and therefore do not change as we go from one time interval to the next) the eigenvectors do change.

The discussion on the size of the different parameters done in section II and also in this section indicates that the effect from the cold axion background is actually the dominant one for Peccei-Quinn axions, well and above the effects due to the presence of the magnetic field. Unfortunately both are minute. In the limit where the magnetic field can be neglected, the photon proper frequencies are

$$\omega_{\pm}^2 = k^2 \pm k\eta_0 \quad (22)$$

Axion-like particles are not constrained by the PCAC relation $f_a m_a \simeq \text{constant}$ required of Peccei-Quinn axions and using (somewhat arbitrarily) the largest value of b discussed and the smallest mass for m_a we get a value for b^2/m_a^2 in the region $\sim 10^{-18}$, to be compared with the largest acceptable value for η_0 that gives $\eta_0/k \sim 10^{-20}$ if $k \sim 1$ eV. Sensitivity to the magnetic field could be enhanced by being able to reproduce the experiment with even larger magnetic fields.⁶

⁵ Ellipticity is the ratio of the minor to major axes of the ellipse.

⁶ Non-destructive magnetic fields close to 100 T have been achieved. This would enhance the sensitivity by a factor 100.

V. CHANGE OF THE POLARIZATION IN AN AXION BACKGROUND

For our purposes it will be useful to consider the electric field correlator, easily derived from the resummed photon propagator derived in Ref. [26]. Using that $\vec{k} \cdot \vec{B} = 0$, we get in momentum space

$$D_{ij}^E(\omega, k) = -\frac{ig_{ij}\omega^2}{\omega^2 - k^2} - \frac{i\omega^4 b_i b_j}{(\omega^2 - k^2)[(\omega^2 - k^2)(\omega^2 - k^2 - m_a^2) - \omega^2 b^2]}. \quad (23)$$

Notice the rather involved structure of the dispersion relation implied in the second term, which is only present when $b \neq 0$, while the first piece corresponds to the unperturbed propagator. For a given value of the wave-number k the zeros of the denominator are actually the proper frequencies ω_a, ω_1 and ω_2 . We consider the propagation of plane waves moving in the \hat{x} direction. The Fourier transform with respect to the spatial component will describe the space evolution of the electric field. We decompose

$$\frac{1}{(\omega^2 - k^2)[(\omega^2 - k^2)(\omega^2 - k^2 - m_a^2) - \omega^2 b^2]} = \frac{A}{k^2 - \omega^2} + \frac{B}{k^2 - F^2} + \frac{C}{k^2 - G^2}, \quad (24)$$

where ω , F and G are the roots of the denominator

$$\begin{aligned} F^2 &= \omega^2 - \frac{m_a^2}{2} + \frac{1}{2}\sqrt{m_a^4 + 4\omega^2 b^2} \approx \left(1 + \frac{b^2}{m_a^2}\right)\omega^2, \\ G^2 &= \omega^2 - \frac{m_a^2}{2} - \frac{1}{2}\sqrt{m_a^4 + 4\omega^2 b^2} \approx \left(1 - \frac{b^2}{m_a^2}\right)\omega^2 - m_a^2, \end{aligned} \quad (25)$$

and

$$\begin{aligned} A &= -\frac{1}{\omega^2 - F^2} \frac{1}{\omega^2 - G^2} = \frac{1}{\omega^2 b^2}, \\ B &= -\frac{1}{F^2 - \omega^2} \frac{1}{F^2 - G^2} \approx -\frac{1}{\omega^2 b^2} \left(1 - \frac{\omega^2 b^2}{m_a^4}\right), \\ C &= -\frac{1}{G^2 - \omega^2} \frac{1}{G^2 - F^2} \approx -\frac{1}{m_a^4}. \end{aligned} \quad (26)$$

The last contribution to B in the previous formula was incorrectly neglected in our previous publication [26]. The space Fourier transform of the electric field propagator is

$$\begin{aligned} D_{ij}^E(\omega, x) &= -g_{ij} \frac{\omega}{2} e^{i\omega x} + \frac{\omega^4}{2} b_i b_j \left(\frac{A}{\omega} e^{i\omega x} + \frac{B}{F} e^{iF x} + \frac{C}{G} e^{iG x} \right) \\ &= \frac{\omega}{2} e^{i\omega x} \left[-g_{ij} + \omega^3 b_i b_j \left(\frac{A}{\omega} + \frac{B}{F} e^{i(F-\omega)x} + \frac{C}{G} e^{i(G-\omega)x} \right) \right], \end{aligned} \quad (27)$$

where x is the travelled distance. After factoring out the exponential $e^{i\omega x}$ we consider the relative magnitude of the differential frequencies $F - \omega$ and $G - \omega$. The latter is much larger

and for $m_a^2 x / 2\omega \gg 1$ the corresponding exponential could be dropped. This approximation was made in Ref. [26] and for the range of axion masses envisaged here and $\omega \sim 1$ eV is valid for all astrophysical and most terrestrial experiments. As for the exponential containing $F - \omega$, we can safely expand it for table-top experiments and retain only the first non-trivial term. In this case, the leading terms in the propagator are

$$D_{ij}^E(\omega, x) \approx \frac{\omega}{2} e^{i\omega x} \left[-g_{ij} + \hat{b}_i \hat{b}_j \left(\frac{\omega^2 b^2}{m_a^4} - i \frac{\omega b^2 x}{2m_a^2} \right) \right], \quad (28)$$

where \hat{b} is a unitary vector in the direction of the magnetic field. For very light axion masses, neglecting the $e^{i(G-\omega)x}$ exponential cannot be justified for table top experiments. Then one should use a slightly more complicated propagator, namely

$$D_{ij}^E(\omega, x) \approx \frac{\omega}{2} e^{i\omega x} \left\{ -g_{ij} + \hat{b}_i \hat{b}_j \frac{\omega^2 b^2}{m_a^4} \left[1 - \cos \frac{m_a^2 x}{2\omega} + i \left(\sin \frac{m_a^2 x}{2\omega} - \frac{m_a^2 x}{2\omega} \right) \right] \right\}. \quad (29)$$

These expressions agree in the appropriate limits with the ones in Ref. [29].

When a CAB is considered the electric field propagator changes to

$$D_{ij}^E(\omega, k) = -i\omega^2 \left(\frac{P_{+ij}}{\omega^2 - k^2 - \eta_0 k} + \frac{P_{-ij}}{\omega^2 - k^2 + \eta_0 k} \right) - i\omega^4 \frac{b_i b_j}{(\omega^2 - k^2)[(\omega^2 - k^2)(\omega^2 - k^2 - m_a^2) - \omega^2 b^2]}. \quad (30)$$

The P_+ and P_- are projectors defined in Ref. [36]. This expression differs from the one presented in formula (75) of Ref. [26] in that (a) only the leading contribution to the term proportional to the magnetic field is retained and (b) the piece independent of the magnetic field contains (unlike in Ref. [26]) the modifications from the CAB. See the appendix for a complete discussion. The external magnetic field can be set to zero in the previous expressions, if desired.

By projecting on suitable directions and taking the modulus square of the resulting quantity, the following expression for the angle of maximal likelihood (namely, the one where it is more probable to find the direction of the rotated electric field) as a function of the distance x can be found

$$\alpha(x) = \beta - \frac{\eta_0 x}{2} - \frac{\epsilon}{2} \sin 2\beta, \quad (31)$$

where β is the initial angle that the oscillation plane of the electric field forms with the background magnetic field and

$$\epsilon \approx -\frac{\omega^2 b^2}{m_a^4} \left(1 - \cos \frac{m_a^2 x}{2\omega} \right). \quad (32)$$

From the results in the appendix, the ellipticity turns out to be

$$e = \frac{1}{2} |\varphi \sin 2\beta|, \quad \varphi \approx \frac{\omega^2 b^2}{m_a^4} \left(\frac{m_a^2 x}{2\omega} - \sin \frac{m_a^2 x}{2\omega} \right). \quad (33)$$

For small distances, $\frac{m_a^2 x}{2\omega} \ll 1$ we can expand the trigonometric functions to get

$$\epsilon \approx -\frac{b^2 x^2}{8}, \quad \varphi \approx \frac{m^2 b^2 x^3}{48\omega}. \quad (34)$$

If this limit is not valid, we have instead

$$\epsilon \approx -\frac{\omega^2 b^2}{m^4}, \quad \varphi \approx \frac{\omega b^2 x}{2m^2}. \quad (35)$$

It can be noted that the effect of the magnetic field always comes with the factor $\sin 2\beta$, which means that it disappears if the electric field is initially parallel ($\beta = 0$) or perpendicular ($\beta = \pi/2$) to the external magnetic field.

The results of Ref. [29], which we reproduce in the case where $\eta_0 = 0$, are known to be in agreement with later studies such as Ref. [33], which has somehow become a standard reference in the field. However, their approach is not adequate to deal with time dependent backgrounds and therefore it is not easy to reinterpret the results derived in the present work when a non-vanishing CAB is present in the language of Ref. [33].

VI. MEASURING THE CAB IN POLARIMETRIC EXPERIMENTS

If $\eta_0 \neq 0$ a rotation is present even in the absence of a magnetic field. This is a characteristic footprint of the CAB. This ‘anomalous’ rotation attempts to bring the initial polarization plane to agree with one of the two elliptic eigenmodes. In the case where the effect of η_0 dominates, the eigenmodes are almost circularly, rather than linearly, polarized so the changes in the plane of polarization could be eventually of order one. The effect is independent of the frequency. Equation (31) shows however that the process of rotation due to the CAB is very slow, with a characteristic time η_0^{-1} .

Typically in interferometric-type experiments the laser light is made to bounce and folded many times. Formula (31) can be used each time that the light travels back and forth. When this happens, β changes sign and so does $\sin 2\beta$. Since ϵ is always negative, the effect of the magnetic field is always to increase β in absolute value (i.e. moving the polarization plane away from the magnetic field). So in this sense, the rotation accumulates. The situation is

different for the CAB term. It does not change sign when β does, so its effect compensates each time the light bounces. However, recall that η_0 changes sign with a half-period πm_a^{-1} so the effect could be accumulated by tuning the length between each bounce. The range of values of πm_a^{-1} makes this perhaps a realistic possibility for table-top experiments (we are talking here about separations between the mirrors ranging from millimeters to meters for most accepted values of m_a).

It turns out that for Peccei-Quinn axions the effect is actually independent both of the actual values for f_a and m_a and it depends only on the combination $f_a m_a \simeq 6 \times 10^{15} \text{ eV}^2$ and the local axion density. Assuming that the laser beam travels a distance $L = \pi m_a^{-1}$ before bouncing, the total maximum rotation that can be observed will be given by $|\eta_0|x$. The total travelled distance will be $x = \mathcal{N}L$, where \mathcal{N} is the total number of turns that depends on the finesse of the resonant cavity. Replacing the expression for $|\eta_0|$ in the previous expression in terms of the local DM density ρ (that we assume to be 100% due to axions) we get $|\eta_0| = g_{a\gamma\gamma} \frac{4\alpha}{\pi^2} \frac{\sqrt{2\rho}}{f_a}$. Then

$$|\eta_0|x = g_{a\gamma\gamma} \frac{4\alpha}{\pi} \frac{\sqrt{2\rho}}{6 \times 10^{15} \text{ eV}^2} \mathcal{N} \simeq 2 \times 10^{-18} \text{ eV}^{-2} \times \sqrt{\rho} \times \mathcal{N}. \quad (36)$$

Plugging in the expected value for the local axion density one gets for every bounce an increment in the angle of rotation of 2×10^{-20} . This is of course a very small number and we realize that the chances of being able to measure this anytime soon are slim. At present there are cavities whose reflection losses are below 1 ppm[41] but these numbers still fall short. However this result may be interesting for several reasons. First of all, it is actually independent from the axion parameters, as long as they are Peccei-Quinn axions, except for the dependence on $g_{a\gamma\gamma}$ that is certainly model dependent but always close to 1. Second, in this case it depends directly on the local halo density and nothing else. Third, a positive result obtained by adjusting the length of the optical path would give an immediate direct measure of m_a and an indirect one of f_a . There are no hidden or model dependent assumptions, the only ingredient that is needed is QED.

Observing a net rotation of the initial plane of polarization when the magnetic field is absent (or very small) would be a clear signal of the collective effect of a CAB. On the contrary, a non-zero value for η_0 does not contribute at leading order to a change in the ellipticity (and subleading corrections are very small). In Ref. [42] the authors discuss in some detail the different backgrounds, all of which are very small with the exception of the

dichroism originating from the experimental apparatus itself [43]. Ways of partially coping with these experimental limitations are discussed in the previous reference.

Notice that the effect is directly proportional to the distance travelled and therefore any improvement in the finesse of the cavity directly translates into a longer distance and a better bound. Recall that in order to measure the rotated angle it is actually much better not to consider an external magnetic field, making the experimental setup much easier. Incidentally this also liberates us from the non-linear QED effects discussed in section II.

Axion-like particles not constrained by the Peccei-Quinn relation $f_a m_a \simeq \text{constant}$ could be easier to rule out if they happen to be substantially lighter than their PQ counterparts as cavities in this case can be longer and one could have longer accumulation times.

VII. CONCLUSIONS

In this work we have extended the analysis of axion-photon mixing in the presence of an external magnetic field to the case where a cold axion background (CAB) is present too. The mixing is then substantially more involved and the two photon polarizations mix even without a magnetic field. In particular in our results we can take the limit where the magnetic field vanishes, a situation that would make experiments easier even if it would be really challenging to measure the predicted effects. Together with resonant cavity experiments, such as ADMX, optical experiments or observations are so far the only ones that appear eventually capable of testing the nature of the CAB.

We have made one approximation that we believe is not essential, namely we have approximated the assumed sinusoidal variation in time of the CAB by a piece-wise linear function; resulting in a fully analytically solvable problem. We believe that this captures the basic physics of the problem and we expect only corrections of $\mathcal{O}(1)$ in some numerical coefficients but no dramatic changes in the order-of-magnitude estimates.

The existence of some momentum gaps due to the periodic time dependence of the CAB and its implications has been reviewed too. It seems challenging to design experiments to verify or falsify their existence, but in any case they are unavoidable if dark matter is explained in terms of an axion background; in fact it would possibly be the most direct evidence of the existence of a CAB.

We have obtained the proper modes and their ellipticities and we have analyzed in detail

the evolution of the system. It should be said that CAB-related effects dominate in some regions of the allowed parameter space. We have also studied the possible presence of accumulative effects that might enhance the rotation of the instantaneous plane of polarization. This would also be a genuine CAB effect.

In order to analyze the evolution of the system we have made use of the two point function for the electric field, that correlates the value at $x = 0$ with the one at a given value for x . We find this a convenient and compact way of treating this problem. It is valuable to have this tool at hand as the propagator encompasses all the information of the travelling photons.

Of course the most relevant question is whether laser experiments may one day shed light on the existence and properties of the CAB. The present authors are not competent to judge on the future evolution of the precision in this type of experiments. In both cases the required precision is several orders of magnitude beyond present accuracy, but progress in this field is very fast.

Apart from the precision issue, there are several caveats to take into account when attempting to experimentally test the predictions of the present work. For instance, a scan on m_a (i.e. the mirror separation) has to be performed until a cumulative effect is found, which obviously takes time (this is in a sense somewhat equivalent to the scan on the resonant frequency of the cavity in ADMX). The total number of reflections is limited by mirror quality (finesse) and it typically induces a spurious rotation that needs to be disentangled from the true effect. We do not think that any of the approximations made in this work (basically the piecewise linear approximation for the CAB profile) is experimentally significant provided that the coherence length of the CAB is larger than the spatial region experimentally probed.

As emphasized in the introduction, checking the coherence of a putative cold axion background is not easy because the physical effects associated to it are subtle and small in magnitude. The present proposal analyzes the consequences of the existence of a CAB on photon propagation and as we have seen its effects can be of a size comparable to other phenomena that are being actively investigated in optical experiments. For these reasons we believe it is important to bring the present analysis to the attention of the relevant experimental community.

Acknowledgements

This work is supported by grants FPA2010-20807, 2009SGR502 and Consolider grant CSD2007-00042 (CPAN). A. Renau acknowledges the financial support of a FPU pre-doctoral grant. It is a pleasure to thank several of the participants in the 9th Patras Workshop for discussions. The authors are grateful to G. Cantatore for discussions on polarimetric experiments.

Appendix A: Propagator

Considering only the spatial components, eq. (52) of Ref. [26] becomes:

$$\mathcal{D}^{ij}(\omega, k) = D^{ij} + i\omega^2 \left\{ \frac{b^i b^j}{(k^4 - \eta_0^2 \vec{k}^2)(k^2 - m_a^2) - \omega^2 k^2 b^2} + \frac{i\eta_0 k^2 (b^i q^j - q^i b^j)}{(k^4 - \eta_0^2 \vec{k}^2)[(k^4 - \eta_0^2 \vec{k}^2)(k^2 - m_a^2) - \omega^2 k^2 b^2]} \right\}, \quad (\text{A1})$$

where

$$D^{ij} = -i \left(\frac{P_+^{ij}}{k^2 - \eta_0 |\vec{k}|} + \frac{P_-^{ij}}{k^2 + \eta_0 |\vec{k}|} \right), \quad \vec{q} = (\vec{b} \times \vec{k}) \quad (\text{A2})$$

and the projectors P_\pm have been defined in Ref. [36]. Terms proportional to $k^i k^j$ have been dropped, since we are interested in contracting the propagator with a photon polarization vector. The roots of the denominators are $|\vec{k}| = F_j$, with

$$\begin{aligned} F_{1,2}^2 &= \omega^2 + \frac{\eta_0^2}{2} \mp \frac{\eta_0}{2} \sqrt{4\omega^2 + \eta_0^2} \approx \omega^2 \mp \omega \eta_0, \\ F_{3,4}^2 &= \omega^2 - \frac{m_a^2 - \eta_0^2}{3} + \sqrt{W} (\cos \chi \mp \sqrt{3} \sin \chi), \\ F_5^2 &= \omega^2 - \frac{m_a^2 - \eta_0^2}{3} - 2\sqrt{W} \cos \chi. \end{aligned} \quad (\text{A3})$$

$$\begin{aligned} W &\approx \left(\frac{m_a^2}{3} \right)^2 \left(1 + \frac{3\omega^2 b^2}{m_a^4} \right), \\ \chi &\approx \frac{1}{m_a^2} \sqrt{3} \omega \xi, \\ \xi &\approx \left(1 + \frac{9\omega^2 b^2}{2m^4} \right)^{-1} \sqrt{\eta_0^2 + \left(\frac{\omega b^2}{2m^2} \right)^2 + \left(\frac{\omega^2 b^3}{m_a^4} \right)^2}. \end{aligned} \quad (\text{A4})$$

F_1 and F_2 correspond to the pieces with P_+ and P_- , respectively. The piece proportional to $b^i b^j$ has poles at $F_{3,4,5}^2$ and the last piece contains all five poles. We decompose the

denominators in simple fractions:

$$\frac{1}{(k^4 - \eta_0^2 \vec{k}^2)(k^2 - m_a^2) - \omega^2 k^2 b^2} = \sum_{l=3}^5 \frac{A_l}{\vec{k}^2 - F_l^2}, \quad (\text{A5})$$

with

$$A_l = \frac{-1}{\prod_{m \neq l, 1, 2} (F_l^2 - F_m^2)}, \quad l = 3, 4, 5 \quad (\text{A6})$$

and

$$\frac{k^2}{(k^4 - \eta_0^2 \vec{k}^2)[(k^4 - \eta_0^2 \vec{k}^2)(k^2 - m_a^2) - \omega^2 k^2 b^2]} = \sum_{l=1}^5 \frac{\tilde{A}_l}{\vec{k}^2 - F_l^2}, \quad (\text{A7})$$

with

$$\tilde{A}_l = \frac{-(\omega^2 - F_l^2)}{\prod_{m \neq l} (F_l^2 - F_m^2)}, \quad l = 1, \dots, 5. \quad (\text{A8})$$

Then,

$$\begin{aligned} \mathcal{D}^{ij}(\omega, \vec{k}) = & i \left(\frac{P_+^{ij}}{\vec{k}^2 - F_1^2} + \frac{P_-^{ij}}{\vec{k}^2 - F_2^2} \right) \\ & + i\omega^2 b^2 \left[\hat{b}^i \hat{b}^j \sum_{l=3}^5 \frac{A_l}{\vec{k}^2 - F_l^2} + i\eta_0 (\hat{b}^i \hat{q}^j - \hat{q}^i \hat{b}^j) \sum_{l=1}^5 \frac{|\vec{k}| \tilde{A}_l}{\vec{k}^2 - F_l^2} \right] \end{aligned} \quad (\text{A9})$$

We choose the axes so that

$$\hat{k} = (1, 0, 0), \quad \hat{b} = (0, 1, 0), \quad \hat{q} = (0, 0, -1). \quad (\text{A10})$$

The propagator in position space is, after dropping an overall factor,

$$\begin{aligned} d^{ij}(\omega, x) \approx & (P_+^{ij} + P_-^{ij}) \cos\left(\frac{\eta_0 x}{2}\right) + i(P_+^{ij} - P_-^{ij}) \sin\left(\frac{\eta_0 x}{2}\right) \\ & + \hat{b}^i \hat{b}^j \sum_{l=3}^5 a_l e^{i\alpha_l x} - i(\hat{b}^i \hat{q}^j - \hat{q}^i \hat{b}^j) \sum_{l=1}^5 \tilde{a}_l e^{i\alpha_l x}, \end{aligned} \quad (\text{A11})$$

where

$$a_l = \frac{\omega^3 b^2 A_l}{F_l}, \quad \tilde{a}_l = \omega^3 b^2 \eta_0 \tilde{A}_l, \quad \alpha_l = F_l - \omega. \quad (\text{A12})$$

All the α_l are proportional to η_0 or b^2 , except for $\alpha_5 \approx -\frac{m_a^2}{2\omega}$. Restricting ourselves only to $y - z$ components, we can write $d(\omega, x)$ in matrix form.

$$P_{+j}^i + P_{-j}^i = \begin{pmatrix} 1 & 0 \\ 0 & 1 \end{pmatrix}, \quad (\text{A13})$$

$$i(P_{+j}^i - P_{-j}^i) = \begin{pmatrix} 0 & 1 \\ -1 & 0 \end{pmatrix}, \quad (\text{A14})$$

$$\hat{b}^i \hat{b}_j = \begin{pmatrix} -1 & 0 \\ 0 & 0 \end{pmatrix}, \quad (\text{A15})$$

$$-i(\hat{b}^i \hat{q}_j - \hat{q}^i \hat{b}_j) = \begin{pmatrix} 0 & -i \\ i & 0 \end{pmatrix}. \quad (\text{A16})$$

If we write

$$\sum_l a_l e^{i\alpha_l x} = -(\epsilon + i\varphi), \quad i \sum_l \tilde{a}_l e^{i\alpha_l x} = -(\tilde{\epsilon} + i\tilde{\varphi}), \quad (\text{A17})$$

we have

$$d_j^i(\omega, x) = \begin{pmatrix} \cos \frac{\eta_0 x}{2} + \epsilon + i\varphi & \sin \frac{\eta_0 x}{2} + \tilde{\epsilon} + i\tilde{\varphi} \\ -(\sin \frac{\eta_0 x}{2} + \tilde{\epsilon} + i\tilde{\varphi}) & \cos \frac{\eta_0 x}{2} \end{pmatrix} \quad (\text{A18})$$

Appendix B: Ellipticity and rotation

The quantities appearing in (A18) are

$$\epsilon \approx -\frac{\omega^2 b^2}{m_a^4} \left(1 - \cos \frac{m_a^2 x}{2\omega}\right), \quad \varphi \approx \frac{\omega^2 b^2}{m_a^4} \left(\frac{m_a^2 x}{2\omega} - \sin \frac{m_a^2 x}{2\omega}\right), \quad (\text{B1})$$

while $\tilde{\epsilon}$ and $\tilde{\varphi}$ are both proportional to $b^2 \eta_0$, so they are negligible.

In the limit $\frac{m_a^2 x}{2\omega} \ll 1$ we have

$$\epsilon \approx -\frac{b^2 x^2}{8}, \quad \varphi \approx \frac{m_a^2 b^2 x^3}{48\omega} \quad (\text{B2})$$

whereas if $\frac{m_a^2 x}{2\omega} \gg 1$ the trigonometric functions oscillate rapidly and can be dropped:

$$\epsilon \approx -\frac{\omega^2 b^2}{m_a^4}, \quad \varphi \approx \frac{\omega b^2 x}{2m_a^2}. \quad (\text{B3})$$

Eq. (B2) agrees with eq. 16 of Ref. [29] (although their k^2 in the denominator should be only k , the dimensions do not fit otherwise). Eq. (B3) agrees with their eq. (20,21), at least to second order in b .

If we start with a polarization $\vec{n}_0 = (\cos \beta, \sin \beta)$, after a distance x we have

$$n_x^i = d_j^i(x) n_0^j = \begin{pmatrix} \cos(\beta - \frac{\eta_0 x}{2}) + (\epsilon + i\varphi) \cos \beta \\ \sin(\beta - \frac{\eta_0 x}{2}) \end{pmatrix} \quad (\text{B4})$$

Following section 1.4 of Ref. [44], this vector describes a polarization at an angle

$$\alpha \approx \beta - \frac{\eta_0 x}{2} - \frac{\epsilon}{2} \sin 2\beta \quad (\text{B5})$$

and with ellipticity

$$e = \frac{1}{2} |\varphi \sin 2\beta|. \quad (\text{B6})$$

This ellipticity differs from the one described in Ref. [29] by the factor of $\sin 2\beta$.

Quantum mechanically the quantity that is relevant is not the amplitude itself, but the modulus squared of it. From this, the probability of finding an angle α given an initial angle β will be

$$P(\alpha, \beta) = |\epsilon'_i d^{ij} \epsilon_j|^2 \approx \cos^2 \left(\alpha - \beta + \frac{\eta_0 x}{2} \right) + 2\epsilon \cos \left(\alpha - \beta + \frac{\eta_0 x}{2} \right) \cos \alpha \cos \beta. \quad (\text{B7})$$

The angle of maximum probability, satisfying $\partial_\alpha P(\alpha, \beta) = 0$ is also, to first order,

$$\alpha = \beta - \frac{\eta_0 x}{2} - \frac{\epsilon}{2} \sin 2\beta. \quad (\text{B8})$$

-
- [1] R.D. Peccei and H.R. Quinn, *Phys. Rev. Lett.* **38**, 1440 (1977).
 - [2] S. Weinberg, *Phys. Rev. Lett.* **40**, 223 (1978).
 - [3] F. Wilczek, *Phys. Rev. Lett.* **40**, 279 (1978).
 - [4] L. Abbott and P. Sikivie, *Phys. Lett. B* **120**, 133 (1983).
 - [5] M. Dine and W. Fischler, *Phys. Lett. B* **120**, 137 (1983).
 - [6] J. Preskill, M.B. Wise and F. Wilczek, *Phys. Lett. B* **120**, 127 (1983).
 - [7] M. Kuster, G. Raffelt and B. Beltran (eds.), *Lecture Notes in Physics* **741**, (2008).
 - [8] P. Sikivie and Q. Yang, *Phys. Rev. Lett.* **112**, 068103 (2009).
 - [9] M. Dine, W. Fischler and M. Srednicki, *Phys. Lett. B*, **104**, 199 (1981).
 - [10] A.R. Zhitnitsky, *Sov. J. Nucl. Phys.* **31**, 260 (1980).
 - [11] J. E. Kim, *Phys. Rev. Lett.* **43**, 103 (1979).
 - [12] M. A. Shifman, A. I. Vainshtein and V. I. Zakharov, *Nucl. Phys. B* **166**, 493 (1980).
 - [13] Particle Data Group (J. Beringer *et al.*), *Phys. Rev. D* **86**, 010001 (2012).
 - [14] A.H. Corsico *et al.*, *JCAP* **1212**, 010 (2012).
 - [15] CAST Collab. (E. Arik *et al.*), *J. Cosmo. Astropart. Phys.* **02**, 008 (2009).
 - [16] IAXO Collab. (I. G. Irastorza *et al.*), *JCAP* **1106**, 013 (2011).
 - [17] ALPS Collab. (R. Bähre *et al.*), *JINST* **1309**, T09001 (2013).
 - [18] ADMX Collab. (S. J. Asztalos *et al.*), *Nuclear Instruments and Methods in Physics Research A* **656**, 39-44 (2011).

- [19] S. M. Carroll, G. B. Field and R. Jackiw, *Phys. Rev. D* **41**, 1231 (1990).
- [20] D. Harari and P. Sikivie, *Phys. Lett. B* **289**, 67 (1992).
- [21] A. Lue, L. M. Wang and M. Kamionkowski, *Phys. Rev. Lett.* **85**, 1506 (2000).
- [22] M. Pospelov, A. Ritz and C. Skordis, *Phys.Rev.Lett.* **103**, 051302 (2009).
- [23] A. Arvanitaki *et al.*, *Phys.Rev. D* **81** 123530 (2010).
- [24] A. A. Andrianov, D. Espriu, F. Mescia and A. Renau, *Phys. Lett. B* **684** 101 (2010).
- [25] D. Espriu, F. Mescia and A. Renau, *JCAP* **1108**, 002 (2011).
- [26] D. Espriu and A. Renau, *Phys. Rev. D* **85**, 025010 (2012).
- [27] S. Adler, *Ann. Phys (NY)* **67**, 599 (1971).
- [28] G. Raffelt and L. Stodolsky, *Phys. Rev. D* **37**, 1237 (1988).
- [29] L. Maiani, R. Petronzio and E. Zavattini, *Phys. Lett. B* **175**, 359 (1987)
- [30] D. Espriu and A. Renau, in *Proceedings of the 9th Patras Workshop*, (Mainz, June 2013) [arXiv:1309.6948].
- [31] H. Euler and B. Kochel, *Naturwiss.* **23**, 246 (1935).
- [32] W. Heisenberg and H. Euler, *Z. Phys.* **98**, 718 (1936).
- [33] G. Raffelt and L. Stodolsky, *Phys. Rev. D* **37**, 1237 (1988).
- [34] See e.g. G. Bertone (ed.), *Particle Dark Matter: Observations, Models and Searches*, Cambridge University Pres (2010).
- [35] PVLAS Collab. (G. Zavattini *et al.*), *Phys. Rev. D* **78**, 032006 (2008).
- [36] A. A. Andrianov, D. Espriu, P. Giacconi and R. Soldati, *JHEP* 0909:057 (2009).
- [37] C. Eisele, A. Y. Nevsky and S. Schiller, *Physical Review Letters* **103**, 090401 (2009).
- [38] S. Herrmann *et al.*, *Physical Review D* **80**, 105011 (2009).
- [39] PVLAS Collab. (G. Zavattini *et al.*) *Int. J. Mod. Phys. A* **27**, 1260017 (2012).
- [40] H. Tam and Q. Yang, *Phys. Lett. B* **716**, 435 (2012).
- [41] A. Muller *et al.*, *Opt. Lett.* **35** (13), 2293 (2010)
- [42] M. Ahlers, J. Jaeckel and A. Ringwald, *Phys. Rev. D* **79**, 075017 (2009).
- [43] G. Zavattini *et al.*, *Applied Physics B - Lasers and Optics* **83**, 571 (2006).
- [44] M. Born and W. Wolf, *Principles of Optics*, 4th edn. (Pergamon Press, Oxford 1970).